GLOBAL JOURNAL OF ENGINEERING SCIENCE AND RESEARCHES

ELECTRICAL PROPERTIES OF COW AND SHEEP'S BONES

Sawsan Ahmed Elhouri Ahmed[*1] & Mubarak Dirar Abdallah[2]
[*1]University of Bahri-College of Applied & Industrial Sciences-Department of Physics-Khartoum - Sudan
[2]Sudan University of Science & Technology-College of Science-Department of Physics & International University of Africa- College of Science-Department of Physics -Khartoum-Sudan

ABSTRACT

In this work five samples of (cow and sheep's bones) were prepared to powders in a period of crashing (10 up to 50 sec); weight = 56.73mg
To find values of:
1. Refractive index
2. Energy gap
3. And Electrical Conductivity

I. INTRODUCTION

Many organic compounds such as polyacetylene $[(CH_2)n]$ and polydiacetylene are semiconductors. Although organic semiconductors are not yet used in any electronic devices, they hold great promise for future applications. The advantage of organic over inorganic semiconductors is that they can be easily tailored to the applications. For example, compounds containing conjugate bonds such as –C=C–C= have large optical nonlinearities and therefore may have important applications in electronics. The band gaps of these compounds can be changed more easily than those of inorganic semiconductors to suit the application by changing their chemical formulas. Recently new forms of carbon, such as C60 (fullerene), have been found to be semiconductors. One form of carbon consists of sheets of graphite rolled into a tube of some nanometers in diameter known as *nanotubes* [1]. These carbon nanotubes and their "cousin", BN nanotubes, hold great promise as nanoscale electronic circuit elements. They can be metals or semiconductors depending on their pitch. The mechanisms by which organic semiconductors conduct electrons cannot be easily described in the same way those inorganic semiconductors have been which is through band theory. According to band theory, the highest occupied energy levels of an atom in a lattice form a valence band and the lowest unoccupied electronic levels form the conduction band; electrical conductivity in semiconductors arises when the band gap between these two bands is small enough for an electron to move from the valence band to the conduction band under excitation. Through the introduction of defects, by doping, additional energy levels can be introduced between the valence and conduction bands reducing the band gap. Insulators have a wide band gap which cannot be crossed whereas full conductors do not possess a band gap and the valence and conduction bands overlap. Over the last two decades, many examples of organic conducting polymers have been demonstrated, however most require an external species, a dopant, to increase conductivities from regimes as low as 10^{-8} S cm^{-1} in undoped polymers to as high as 10^4 S cm^{-1} in doped semiconductors. By controlling the concentration of dopants in a material it is possible to tune the conductivity of a polymer. Unlike inorganic semiconductors, in which an impurity is introduced to a crystalline semiconductor to reduce the gap between the valence and conduction bands, doping in organic semiconductors requires the addition of strongly electron donating (n-type) or strongly electron withdrawing (p-type) molecular species which induce mobile charge carriers along the polymer backbone. A p-type dopant can be thought of as an oxidizing agent which removes an electron from the highest occupied molecular orbital (HOMO) of the organic semiconductor, introducing a positive hole along the backbone. An n-type dopant on the other hand, is a reducing agent which donates an electron to the lowest unoccupied molecular orbital (LUMO) of the organic semiconductor introducing a negative charge carrier[2]. The integer charge transfer model and the molecular orbital levels involved in the doping processes (p-type and n-type) are schematically represented in this Fig.
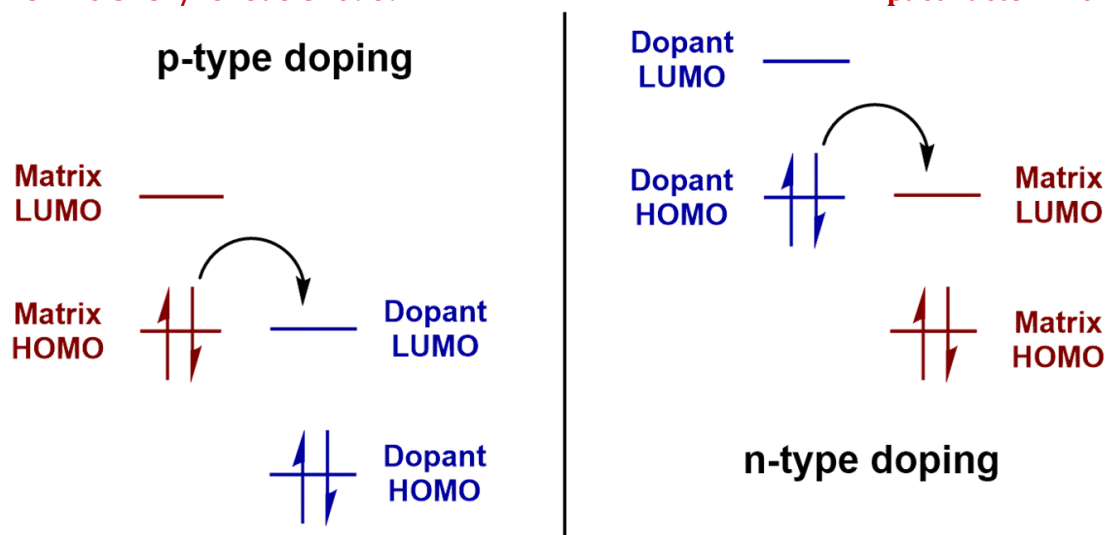
Fig. (1.1): Organic semiconductor doping via integer charge transfer model.

More recently it has emerged however that the integer charge transfer model is a simplified model to describe the doping in organic semiconductors. A more accurate description of organic semiconductor doping is described in the hybrid charge transfer model. In contrast to the discrete energy levels involved in the integer charge transfer model, the hybrid charge transfer model describes the doping of organic semiconductors via the formation of charge transfer states arising from orbital mixing between donor and acceptor orbital's [2]. For a more comprehensive discussion on the hybrid charge transfer model and doping in organic semiconductors, the reader is referred to another review if required. Some of the earliest examples of conducting organic materials come from the p-type doping of polyacetylene with halogens. In those early conducting polymers, dopants were introduced via exposure to halogen vapors leading to diffusion problems during processing. A more common and practical approach is to use small molecules as dopants. P-type doping has been widely explored with strong Lewis acids being employed [3]. N-doping of materials is much more difficult to achieve since the HOMO of the dopant must be high to allow it to donate electrons to the LUMO of various materials, however having such a high-energy HOMO makes the dopant more resistive to the oxidation it is required to undergo. N-doping has previously been achieved using alkali metals, mostly lithium, and molecules with extremely high HOMO levels such as tetrathianaphthacene (TTN, EHOMO = -4.7 eV), which doped hexadecafluoro-zinc-phthalocyanine ($F_{16}ZnPc$) with a LUMO energy level of -4.5 eV. The same dopant however did not dope tris(8-hydroxyquinoline)aluminum (Alq_3) with a LUMO energy level of -2.5 eV, showing that similar energies in the HOMO of the dopant and LUMO of the acceptor are essential. In p-type doping the polymer is oxidized by the dopant this produces a positive cation and a free radical electron on the polymer, the charge neutrality is maintained by the formation of an anion on the reduced dopant. If this process occurs twice in *trans*-polyacetylene for example (Figure 1.1), the two radical electrons can recombine to form what is known as a spineless solution, a positive or negative charge carrier free to independently move around the polymer chain. The process of forming solutions is unique to *trans*-polyacetylene due to it containing a doubly degenerate ground state which allows the solitons charges to move independently of each other. Most conjugated polymers however do not exhibit the same symmetry as *trans*-polyacetylene and therefore do not contain the degenerate ground state necessary for independent solitons to act as charge carriers. Considering p-type doping, an electron is removed from the polymer and the cation and radical are again formed; the resultant cation and radical electron are partially delocalized over the π-conjugated system and is termed a polaron (Figure 1.2). The polaron induces the formation of the quinoid structure leading to a distortion in bond lengths over the section of the polymer linking the radical and cation. This distortion is not energetically favored and is therefore usually stabilized over more than one monomer unit. Upon further oxidation, which can be induced by increasing dopant concentration, the unpaired radical electron of the polaron can be removed which leads to a sequence of quinoid type monomer units along the polymer which are separated from the normal aromatic monomer units by the two cationic charges. These sections of the polymer

are known as bipolarons and at high dopant levels are responsible for charge transport across the polymer [4,5,and 6].
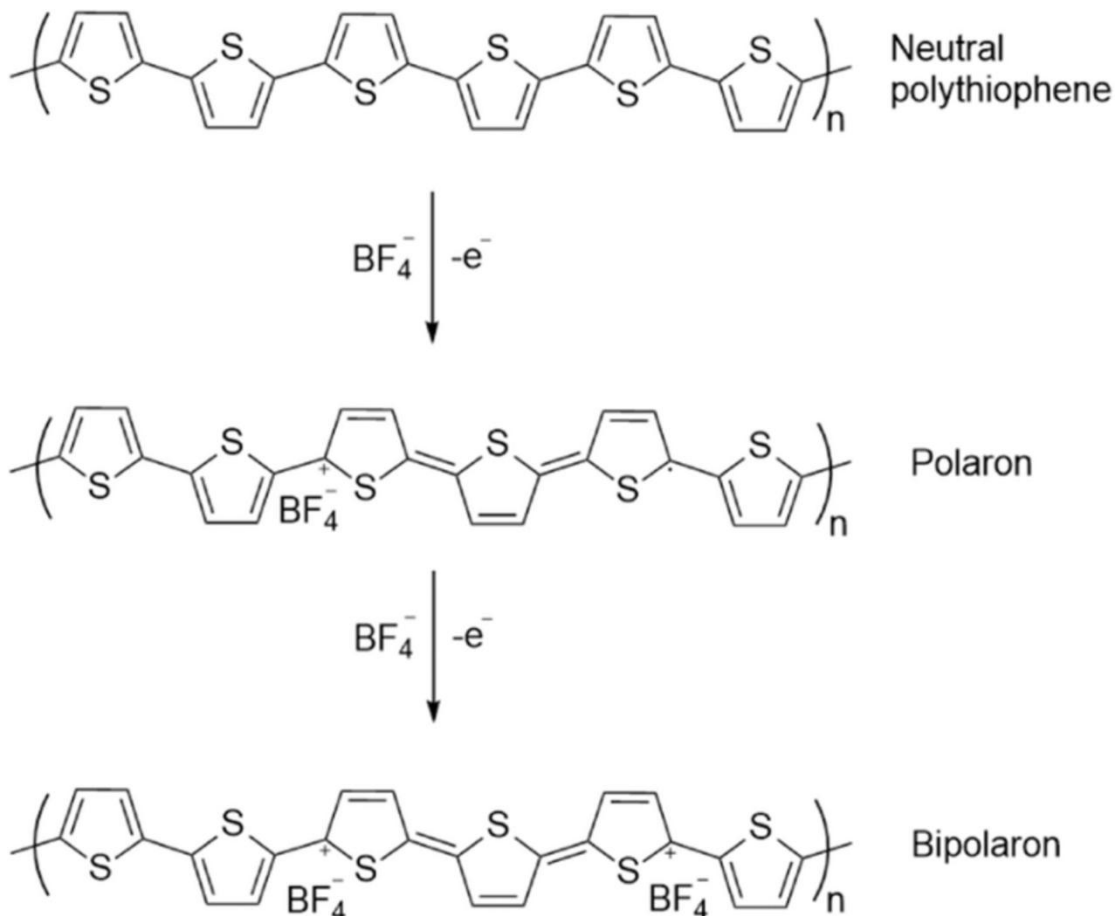
Figure (1.2): Bipolarons formation in polythiophene upon doping with BF4

The organic materials have been explored as the working material the devices, low-cost, flexible, and easily manufactured systems. The same materials also possess features that make them unique in bio-electronics applications, where electronic signals are translated into bio-signals and vice versa. The mechanisms by which organic semiconductors conduct electrons cannot be easily described in the same way those inorganic semiconductors have been which is through band theory. According to band theory, the highest occupied energy levels of an atom in a lattice form a valence band and the lowest unoccupied electronic levels form the conduction band; electrical conductivity in semiconductors arises when the band gap between these two bands is small enough for an electron to move from the valence band to the conduction band under excitation. Through the introduction of defects, by doping, additional energy levels can be introduced between the valence and conduction bands reducing the band gap. Insulators have a wide band gap which cannot be crossed whereas full conductors do not possess a band gap and the valence and conduction bands overlap. Over the last two decades, many examples of organic conducting polymers have been demonstrated, however most require an external species, a dopant, to increase conductivities from regimes as low as 10^{-8} S cm^{-1} in undoped polymers to as high as 10^{4} S cm^{-1} in doped semiconductors. By controlling the concentration of dopants in a material it is possible to tune the conductivity of a polymer. Unlike inorganic semiconductors, in which an impurity is introduced to a crystalline semiconductor to reduce the gap between the valence and conduction bands, doping in organic semiconductors requires the addition of strongly electron donating (n-type) or strongly electron with drawing (p-type) molecular species which induce

3

mobile charge carriers along the polymer backbone. Ap -type dopant can be thought of as an oxidizing agent which removes an electron from the highest occupied molecular orbital (HOMO) of the organic semiconductor, introducing a positive hole along the backbone. An n-type dopant on the other hand, is a reducing agent which donates an electron to the lowest unoccupied molecular orbital (LUMO) of the organic [7,8]. The challenging applications of organic materials for different fields, much more scientists have been prepared organic based materials by novel synthesis and reported functional physical and chemical characteristics of materials for possible applications. Recently (6) Organic materials are effectively used in lamp industry as phosphors for emission of visible light by different excitation energy. Therefore, much work is possible for development of organic efficient phosphors by low cost synthesis for energy saving lamp phosphors, such as solid state lighting [9, 10]. Recently, Cocchi et al. reported highly efficient, variable-color light-emitting diodes (LEDs) realized via mixing of molecular exciton and exciter phosphorescent emissions from a new organic phosphor have been used as either the low-concentration bluish-green.

II.   EXPERIMENTAL SETUP
Apparatus:

Diffuse Reflectance Sampling
Ideal for Powdered Samples and Intractable solids, as well crystalline materials in mid-IR and NIR spectral ranges. One of its benefits that it is an excellent sampling technique as it eliminates the time consuming process of pressing pellets for transmission measurements. It is used to the effects of time and catalysis by configuring the accessory with samples. Perhaps one of the greatest additional benefits is that it is ideally amenable to automation. Also methods can be developed to calculate the electrical conductivity .

USB 2000 spectrometer
The USB2000 Spectrometer connects to a notebook or desktop PC via USB port or serial port. When connected to the USB port of a PC, the USB2000 draws power from the host PC, eliminating the need for an external power supply. Ocean Optics permanently secures all components in the USB2000 at the time of manufacture. Only Ocean Optics Technicians can replace interchangeable components, where noted.
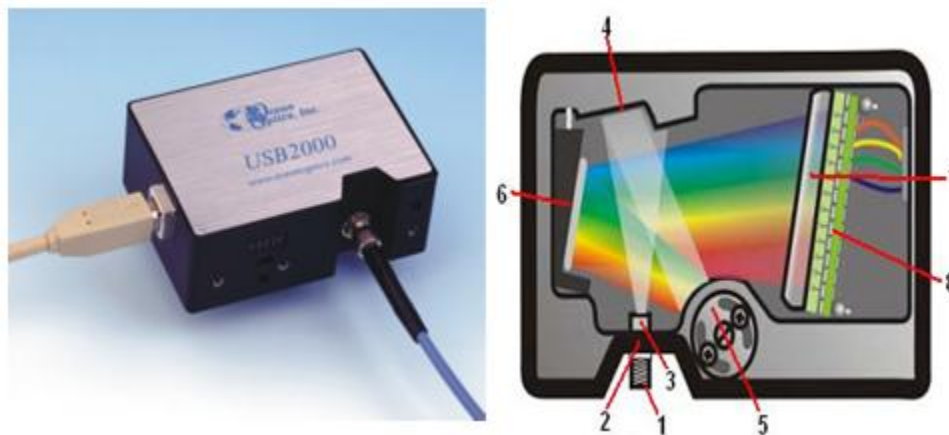
Fig (2.1) Ocean Optics USB2000 Fiber Optic Spectrometer

Fig (2.2) the bones samples using USB2000 device to take the energy gap readings

Item	Name	Description
1	SMA Connector	The SMA Connector secures the input fiber to the spectrometer. Light from the input fiber enters the optical bench through this connector.
2	Slit*	The Slit is a dark piece of material containing a rectangular aperture, which is mounted directly behind the SMA Connector. The size of the aperture regulates the amount of light that enters the optical bench and controls spectral resolution. You can also use the USB2000 without a Slit. In this configuration, the diameter of the fiber connected to the USB2000 determines the size of the entrance aperture. Only Ocean Optics technicians can change the Slit.
3	Filter*	The Filter is a device that restricts optical radiation to pre-determined wavelength regions. Light passes through the Filter before entering the optical bench. Both band pass and long pass filters are available to restrict radiation to certain wavelength regions. Only Ocean Optics technicians can change the Filter.
4	Collimating Mirror	The Collimating Mirror focuses light entering the optical bench towards the Grating of the spectrometer. Light enters the spectrometer, passes through the SMA Connector, Slit, and Filter, and then reflects off the Collimating Mirror onto the Grating.
5	Grating*	The Grating diffracts light from the Collimating Mirror and directs the diffracted light onto the Focusing Mirror. Gratings are available in different groove densities, allowing you to specify wavelength coverage and resolution in the spectrometer. Only Ocean Optics technicians can change the Grating.
6	Focusing Mirror	The Focusing Mirror receives light reflected from the Grating and focuses the light onto the CCD Detector or L2 Detector Collection Lens (depending on the spectrometer configuration).
7	L2 Detector Collection Lens*	The L2 Detector Collection Lens (optional) attaches to the CCD Detector. It focuses light from a tall slit onto the shorter CCD Detector elements. The L2 Detector Collection Lens should be used with large diameter slits or in applications with low light levels. It also improves efficiency by reducing the effects of stray light.

		Only Ocean Optics technicians can add or remove the L2 Detection Collection Lens.
8	CCD Detector (UV or VIS)	The CCD Detector collects the light received from the Focusing Mirror or L2 Detector Collection Lens and converts the optical signal to a digital signal. Each pixel on the CCD Detector responds to the wavelength of light that strikes it, creating a digital response. The spectrometer then transmits the digital signal to the OOIBase32 application

III.   PROCEDURE

Five Samples of (cow and sheep bones) were prepared to powders in a period of crashing (10 up to 50 sec); weight = 56.73mg

The five samples of each type (cow/sheep bones) were replaced on the discs in the USB2000device, to find the values of:
 ➢   Refractive index
 ➢   Energy gap
 ➢   And Electrical Conductivity

The USB 2000 spectrophotometer was used to measurement the diffuse reflectance for the samples prepared. It relies upon the focused projection of the spectrometer beam into the sample where it is reflected, scattered and transmitted through the sample material.

IV.   METHOD OF ANALYSIS

An examples of analysis as in fig (2.1-left), the back reflected, diffusely scattered light (some of which is absorbed by the sample) is then collected by the accessory and directed to the detector optics. Only the part of the beam that is scattered within a sample and returned to the surface is considered to be diffuse reflection. Diluting ensures a deeper penetration of the incident beam into the sample which increases the contribution of the scattered component in the spectrum and minimizes the specula reflection component. The specula reflectance component in diffuse reflectance spectra causes changes in band shapes, their relative intensity, and, in some cases, it is responsible for complete band inversions (Restrahlen bands). Dilution of the sample with a non-absorbing matrix minimizes these effects (particle size and sample loading mechanics also play an important role).

V.   RESULTS AND DISCUSSION:

The USB 2000 spectrophotometer was used to measurement the Diffuse reflectance for the samples prepared to calculated the (Refractive Index , energy gap and Electrical conductivity) for the samples of (cow and sheep Bones) the results were as shown in the fig (5.3 to 5.10).
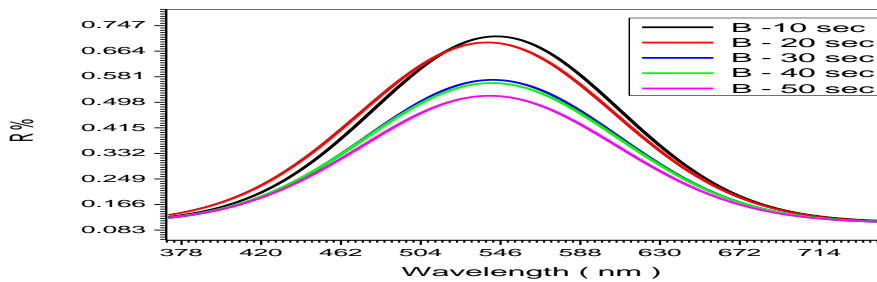
Fig. (5.3). Diffuse reflectance spectra of ibuprofen with and without Kubelka-Monk conversion with (λ) for cow bones samples
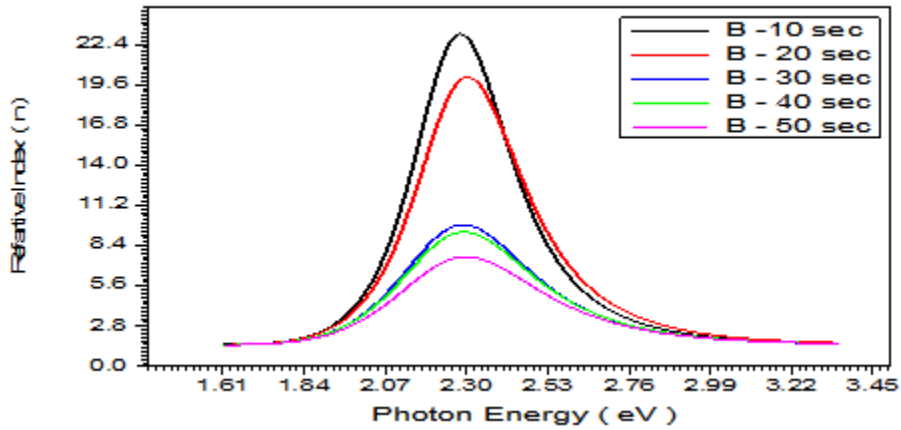
Fig (5.4) the variation of refractive index (n) Vs (hυ) for cow bones samples
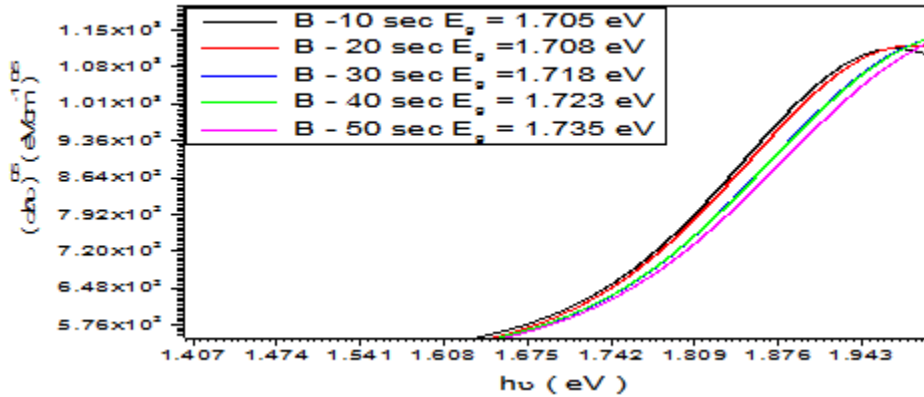
Fig (5.5) the optical energy gap (E_g) value for cow bones samples
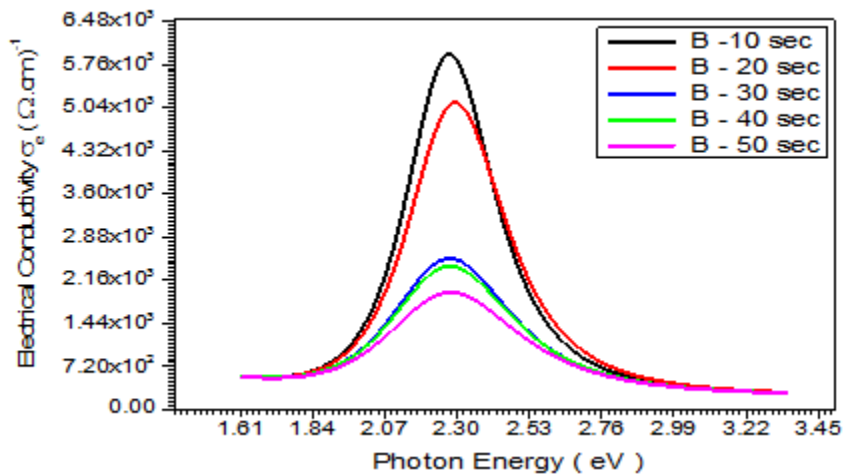
Fig (5.6) the relation between electrical conductivity and photon energy (hυ) for cow bones samples
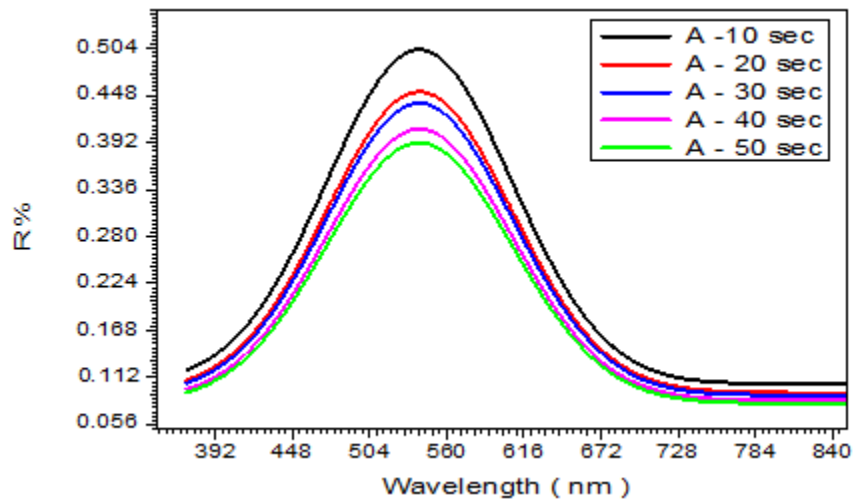
Fig. (5.7). Diffuse reflectance spectra of ibuprofen with and without Kubelka-Monk conversion with (λ) for sheep bones samples
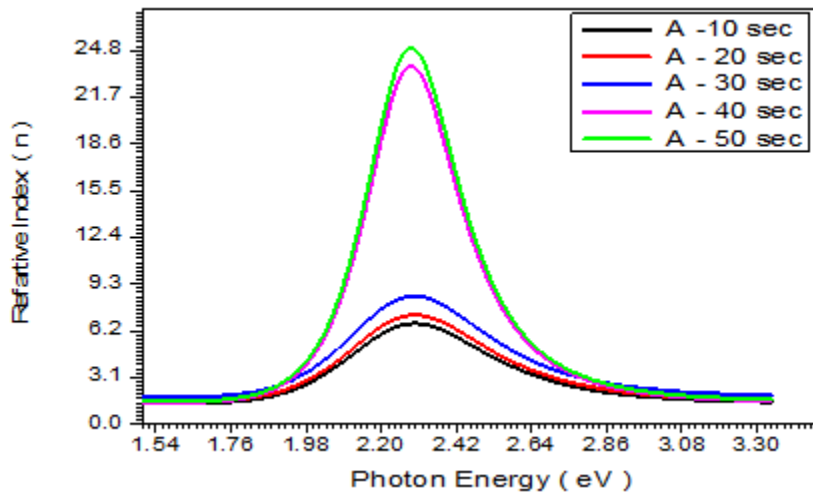
Fig. (5.8) the variation of refractive index (n) with photon energy (hυ) for sheep bones samples
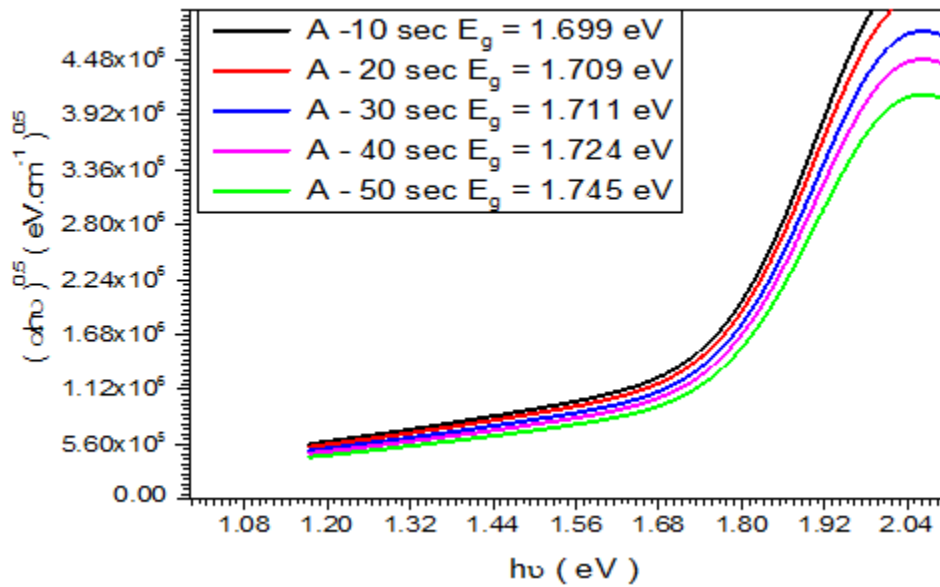
Fig(5.9) Optical energy gab of sheep bones samples
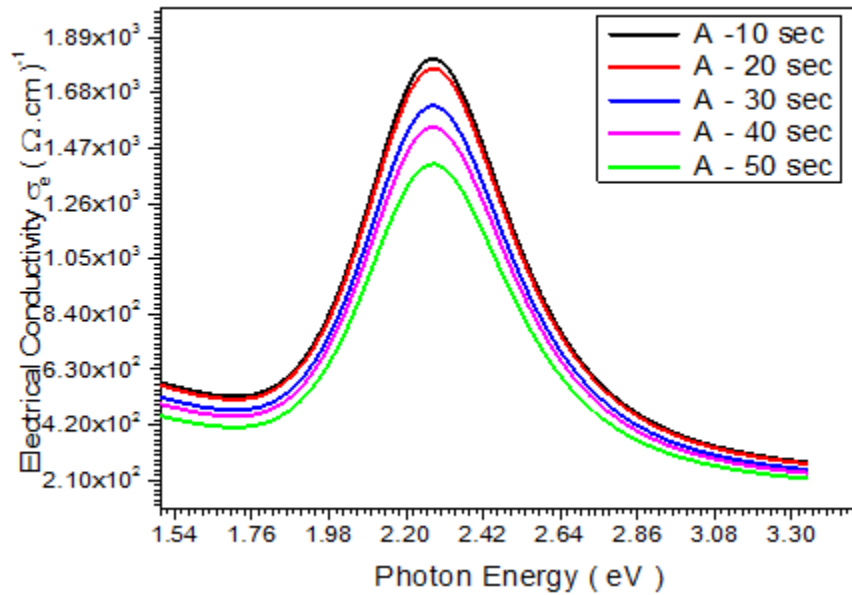
Fig (5.10) the relation between electrical conductivity and photon energy (hυ) for sheep bones

VI.   DISCUSSION

➢   In fig (5.4) show that the reflectance(R) spectra of cow bones. The reflectance of this samples in the ranged (378 –714) nm wavelength. The maximum reflectance of this samples at 540 nm corresponding to photon energy (2.3 eV) then it decreases in the cheep of reflectance when increases the time of the sample.

➢ Fig (5.6) show that the reflectance(R) spectra of sheep bones. The reflectance of this samples in the ranged (390 –730) nm wavelength. The maximum reflectance of this samples at 560 nm corresponding to photon energy (2.2 eV) then it decreases in the cheep of reflectance when increases the time of the sample.

➢ The refractive index (n) is the relative between speeds of light in vacuum to its speed in material which does not absorb this light. The value of n was calculated from the equation

$$n = [\left(\frac{1+R}{1-R}\right)^2 - (1 + k^2)]^{\frac{1}{2}} + \frac{1+R}{1-R}$$

The variation of refractive index (n) Vs (hυ) for cow bones samples are shown in fig.(5.4), which shows that the maximum value of (n) is (22.6) for all cow bones samples at 2.3 eV photon energy . Also the value of refractive index (n) begins to decrease in the region of spectrum while the time of sample crashing increases.

➢ The refractive index (n) is the relative between speed of light in vacuum to its speed in material which does not absorb this light. The value of n was calculated from the equation

$$n = [\left(\frac{1+R}{1-R}\right)^2 - (1 + k^2)]^{\frac{1}{2}} + \frac{1+R}{1-R}$$

The variation of the refractive index (n) Vs (hυ) for sheep bones samples are shown in fig.(5.8), which shows that the maximum value of (n) is (25.34) for all sheep pones samples at 2.3 eV photon energy . Also the values of (n) begin to decrease in the region of spectrum while the time of sample crashing decreases.

➢ The optical energy gap (E_g) has been calculated by the relation

$$(\alpha h\upsilon)^n = C(h\upsilon - E_g)$$

Where (C) is constant. By plotting $(\alpha h\upsilon)^n$ Vs photon energy (hυ) as shown in fig (5.5) for cow bones samples . And by extrapolating the straight thin portion of the curve to intercept the energy axis, the value of the energy gap has been calculated. The value of (E_g) obtained was (1.705) eV, which is approach the value of (1.735) eV reported elsewhere. The value of (Eg) was increased from (1.705) eV to (1.735) eV at sample of 50 sec crashing. The increasing of (E_g) may be related to decrease in grain boundaries and their density due to the time effect of the sample crashing. It was observed that the different structures of the sample confirmed the reason for the band gap shifts.

➢ The optical energy gap (E_g) has been calculated by the relation

$$(\alpha h\upsilon)^n = C(h\upsilon - E_g)$$

where (C) is constant. By plotting $(\alpha h\upsilon)^n$ vs. photon energy (hυ) as shown in fig (5.9) for sheep bones samples . And by extrapolating the straight thin portion of the curve to intercept the energy axis, the value of the energy gap has been calculated. The value of (E_g) obtained was (1.699) eV, which is approach the value of (1.745) eV reported elsewhere. The value of (E_g) was increased from (1.699) eV to (1.745) eV at sample 50 sec crashing . The increasing of (E_g) may be related to decrease in grain boundaries and their density due to the time effect of the sample crashing. It was observed that the different structures of the sample confirmed the reason for the band gap shifts.

➢ The optical conductivity is a measure of frequency response of material when irradiated with light which is determined using the following relation:

$$\delta_{opt} = \frac{\alpha n c}{4\pi}$$

Where(c) is the light velocity. The electrical conductivity can be estimated using the following relation

$$\delta_e = \frac{2\lambda \delta_{0pt}}{\alpha}$$

The high magnitude of electrical conductivity 5968.18 $(\Omega.cm)^{-1}$ confirms the presence of very high photo-response of the cow bones samples. The decreased of electrical conductivity at time of sample crashing is due to the high absorbance of cow bones samples and may be due to electron excitation by photon energy as it is shown in figs. (5.6).

➢ The optical conductivity is a measure of frequency response of material when irradiated with light which is determined using the following relation,

$$\delta_{opt} = \frac{\alpha n c}{4\pi}$$

Where(c) is the light velocity. The electrical conductivity can be estimated using the following relation

$$\delta_e = \frac{2\lambda \delta_{0pt}}{\alpha}$$

The high magnitude of electrical conductivity 1821.14 $(\Omega.cm)^{-1}$ confirms the presence of very high photo-response of the sheep bones samples. The decreased of electrical conductivity at time of sample crashing is due to the high absorbance of sheep bones samples and may be due to electron excitation by photon energy as it is shown in Figs. (5.10).

➢ All results of (refractive Index , energy gap and electrical conductivity) for all samples of (cow and sheep bones) where noted on table (6.1).

Table (6.1) the results of refractive Index, energy gap and electrical conductivity for all samples of (cow and sheep Bones)

Sample cow bones	Time of crashing (sec)	δ_A $(\Omega.cm)^{-1}$	E_g (eV)	Refractive index (n)	Sample sheep bones	δ_B $(\Omega.cm)^{-1}$	E_g (eV)	Refractive index (n)
A1	10	1821.14	1.699	6.570	B1	5968.18	1.705	23.19
A2	20	1777.68	1.709	7.310	B2	5100.88	1.708	20.15
A3	30	1632.82	1.711	8.460	B3	2548.53	1.718	09.95
A4	40	1545.89	1.724	23.66	B4	2399.85	1.723	09.28
A5	50	1401.02	1.745	25.34	B5	1953.81	1.735	07.57

VII. CONCLUSION

❖ 10 Samples of (cow and sheep bones) were prepared to powders in deferent time of crashing (10 ,20 ,30.40 and 50 sec) and got 5 samples of each type and were replaced on the disc of the USB2000device , values of (refractive Index , energy gap and Electrical conductivity) for all samples, were found.

❖ The reflectance(R) spectra of cow bones in the ranged (378 –714) nm wavelength and sheep bones in the ranged (390 –730) and the maximum reflectance of cow bones at 540 nm corresponding to photon energy (2.3 eV) but sheep bones at 560 nm corresponding to photon energy (2.2 eV) , then it decreases in the cheep and cow reflectance when the time of sample crashing increases.

❖ The maximum value of refractive index (n) is (22.6) for all cow bones samples at 2.3 eV photon energy and maximum value of refractive index (n) is (25.34) for all sheep bones samples at the same photon energy .

❖ The value of(E_g) for cow bones samples was increased from (1.705) eV to (1.735) eV and for sheep bones samples was increased from (1.699) eV to (1.745) eV.

❖ The high magnitude of electrical conductivity 5968.18 $(\Omega.cm)^{-1}$ of the cow bones samples but the sheep bones samples is 1821.14 $(\Omega.cm)^{-1}$.

REFERENCES

1. *Feynman, Richard (1963). Feynman Lectures on Physics. Basic Books.*
2. *"Silicon Semiconductor". http://call1.epizy.com/. Retrieved 2017-02-15. External link in |website= (help)*
3. *Shockley, William (1950). Electrons and holes in semiconductors : with applications to transistor electronics. R. E. Krieger Pub. Co. ISBN 0-88275-382-7.*
4. *Neamen, Donald. "Semiconductor Physics and Devices" (PDF). Elizabeth A. Jones.*
5. *By Abdul Al-Azzawi. "Light and Optics: Principles and Practices." 2007. March 4, 2016.*
6. *"How do thermoelectric coolers (TECs) work?". marlow.com. Retrieved 2016-05-07.*
7. *B.G. Yacobi, Semiconductor Materials: An Introduction to Basic Principles, Springer 2003 ISBN 0-306-47361-5, pp. 1–3*
8. *Yu, Peter (2010). Fundamentals of Semiconductors. Berlin: Springer-Verlag. ISBN 978-3-642-00709-5.*

9. *As in the Mott formula for conductivity, see Cutler, M.; Mott, N. (1969). "Observation of Anderson Localization in an Electron Gas". Physical Review.* **181** *(3): 1336. Bibcode:1969PhRv..181.1336C. doi:10.1103/PhysRev.181.1336.*

10. *Charles Kittel (1995) Introduction to Solid State Physics, 7th ed. Wiley, ISBN 0-471-11181-3.*